Neuronal $P2X_7$ Receptors Are Targeted to Presynaptic Terminals in the Central and Peripheral Nervous Systems

Susan A. Deuchars,[1] Lucy Atkinson,[1] Ruth E. Brooke,[1] Hanny Musa,[1] Carol J. Milligan,[1] Trevor F. C. Batten,[3] Noel J. Buckley,[2] Simon H. Parson,[1] and Jim Deuchars[1]

[1]School of Biomedical Sciences, University of Leeds, LS2 9NQ, Leeds, United Kingdom, Schools of [2]Biochemistry and Molecular Biology, and [3]Medicine, University of Leeds, LS2 9JT, Leeds, United Kingdom

The ionotropic ATP receptor subunits $P2X_{1-6}$ receptors play important roles in synaptic transmission, yet the $P2X_7$ receptor has been reported as absent from neurons in the normal adult brain. Here we use RT-PCR to demonstrate that transcripts for the $P2X_7$ receptor are present in extracts from the medulla oblongata, spinal cord, and nodose ganglion. Using *in situ* hybridization mRNA encoding, the $P2X_7$ receptor was detected in numerous neurons throughout the medulla oblongata and spinal cord. Localizing the $P2X_7$ receptor protein with immunohistochemistry and electron microscopy revealed that it is targeted to presynaptic terminals in the CNS. Anterograde labeling of vagal afferent terminals before immunohistochemistry confirmed the presence of the receptor in excitatory terminals. Pharmacological activation of the receptor in spinal cord slices by addition of 2′- and 3′-*O*-(4-benzoylbenzoyl)adenosine 5′-triphosphate (BzATP; 30 μM) resulted in glutamate mediated excitation of recorded neurons, blocked by $P2X_7$ receptor antagonists oxidized ATP (100 μM) and Brilliant Blue G (2 μM). At the neuromuscular junction (NMJ) immunohistochemistry revealed that the $P2X_7$ receptor was present in motor nerve terminals. Furthermore, motor nerve terminals loaded with the vital dye FM1–43 in isolated NMJ preparations destained after application of BzATP (30 μM). This BzATP evoked destaining is blocked by oxidized ATP (100 μM) and Brilliant Blue G (1 μM). This indicates that activation of the $P2X_7$ receptor promotes release of vesicular contents from presynaptic terminals. Such a widespread distribution and functional role suggests that the receptor may be involved in the fundamental regulation of synaptic transmission at the presynaptic site.

Key words: ATP; purine receptor; synaptic transmission; excitatory amino acid transmission; spinal cord; medulla oblongata; neuromuscular junction

In the nervous system, ATP acts as a fast neurotransmitter at excitatory purinergic synapses and activates ligand-gated cationic channels, the P2X receptors (North and Surprenant, 2000). The P2X receptor family consists of seven cloned subtypes, of which $P2X_{1-6}$ have been localized to neurons in the CNS at both presynaptic and postsynaptic sites (Collo et al., 1996; Vulchanova et al., 1997; Le et al., 1998; Llewellyn-Smith and Burnstock, 1998; Loesch and Burnstock, 1998; Atkinson et al., 2000) and have been shown to mediate both postsynaptic responses (Bardoni et al., 1997; Edwards et al., 1997; Nieber et al., 1997; Pankratov et al., 1998) and presynaptic release of neurotransmitters (Gu and MacDermott, 1997; Khakh and Henderson, 1998; Boehm, 1999). In contrast there is no evidence to support the presence of the $P2X_7$ receptor ($P2X_7R$) in neurons in normal adult brain.

The $P2X_7$ receptor subtype has been localized to widespread tissues in the periphery (Afework and Burnstock, 1999; Bardini et al., 2000; Lee et al., 2000; Pannicke et al., 2000) and was previously identified pharmacologically in cells with potential immunological functions as the P2Z receptor (Ralevic and Burnstock, 1998). In many cell types activation of the $P2X_7$ receptor has been associated with cell lysis and death (Surprenant et al., 1996; Rassendren et al., 1997; Chow et al., 1997; Virginio et al., 1999). In the CNS the $P2X_7$ receptor has been reported as absent from neurons but present only in ependymal cells and activated microglia (Collo et al., 1997). This suggests a role in pathophysiology for the $P2X_7$ receptor because ATP can be released in the CNS in response to cell injury (Dubyak and el Moatassim, 1993) or other conditions such as anoxia (Lutz and Kabler, 1997). Furthermore, activation in microglia of a P2 receptor that is likely to be $P2X_7$ results in the production of inflammatory cytokines, which have been associated with progression of neurodegenerative diseases (Hide et al., 2000). Thus, the expression of $P2X_7$ receptor by brain macrophages rather than neurons would be consistent with a role in brain repair after inflammation, infarction, or immune insult

However, in this current work we reveal unexpected findings that indicate a fundamental role for the $P2X_7$ receptor in the process of neuronal synaptic transmission. We report that the receptor is expressed by neurons and is functionally targeted to excitatory presynaptic terminals that are widespread throughout the CNS, as well as at the neuromuscular junction in the peripheral nervous system. Furthermore, the receptor is functionally present because its activation promotes release of vesicular contents from presynaptic terminals in both central and peripheral nervous systems.

Parts of this work have been published in preliminary reports (Deuchars et al., 2000; Knutsen et al., 2000).

Received May 15, 2001; revised July 5, 2001; accepted July 9, 2001.

We thank the British Heart Foundation (S.A.D., H.M., T.F.C.B., J.D.), Wellcome Trust (L.A., C.J.M., N.J.B., J.D.), and Action Research (S.H.P.) for their generous support.

Correspondence should be addressed to Jim Deuchars, School of Biomedical Sciences, University of Leeds, LS2 9NQ, Leeds, UK. E-mail: J.Deuchars@leeds.ac.uk.

MATERIALS AND METHODS

Detection of mRNA encoding the $P2X_7$ receptor. Total cellular RNA was extracted from freshly dissected spinal cord, medulla oblongata, and nodose ganglia using TRI reagent (Sigma, Poole, UK) according to the

manufacturer's instructions. Because the $P2X_7$ receptor has been reported in blood borne cells, we perfused the animal with artificial CSF before removal of tissue. Tissue was dissected from 150–200 gm Wistar rats. Two micrograms of RNA were reverse-transcribed using oligo-dT and mouse murine leukemia virus reverse transcriptase (Promega, Southampton, UK) in a final volume of 20 μl. One microliter aliquots were used for RT-PCR analysis in a 20 μl reaction volume using 500 nM primers, 250 μM deoxynucleotide triphosphates, and 0.2 U/μl taq polymerase (Promega) final concentration.

Cycling conditions were 95°C for 5 min, followed by 35 cycles of 95°C for 30 sec, 57°C for 30 sec, and 72°C for 1 min followed by a final extension step of 72°C for 10 min. Primers used were $P2X_7$ 162s (agacaaacaaagtcacccgg) and $P2X_7$ 562a (ggtatacacctgccggtctgg) and hprt 231s (cctgctggattacattaaagc) and hprt 576a (gaagtactcattatagtcaagg). PCR products were separated by electrophoresis through a 2% agarose gel.

In situ *hybridization.* Rats were anesthetized with intraperitoneal Sagatal (60 mg/ml; Rhone Merieux, Essex, UK) and perfused transcardially with sucrose containing artificial CSF. Sections were cryostat cut at 10 μm, mounted on slides that had been pretreated with 3-aminopropyltriethoxysilane (Sigma), and stored at −80°C until use. A 200 bp cDNA fragment of the $P2X_7$ receptor corresponding to bases from 127 to 328 (numbering according to GenBank accession number X95882) was cloned into pGEM T-easy (Promega) and used to generate digoxigenin (DIG)-labeled sense and antisense RNA probes. *In situ* hybridization was performed by a modified version of the manufacturer's protocol. The sections were mounted in Aquamount and were viewed on a Nikon E600 microscope.

Western blot analysis. The primary antibody was raised in rabbit against residues 576–595 of rat $P2X_7$ receptor with additional N-terminal cysteine (anti-$P2X_7$ receptor; Alomone Labs, Jerusalem, Israel). Specificity was determined by Western blot analysis. Rat brainstem and spinal cord were separately isolated and crushed under liquid nitrogen. Tissue was resuspended in homogenization buffer [500 μl of protease inhibitor (1 mM iodoacetamide, 1 mM benzathonium chloride, and 5.7 mM PMSF in 5 ml of 1% SDS), 10 mM EDTA, 300 mM sucrose in 4.5 ml of 1% SDS] and centrifuged at 10000 rpm for 3–4 min until a clear pellet and supernatant could be defined. Tissue proteins (30 μg) were separated by SDS-PAGE using 10% acrylamide gels in a Bio-Rad (Hercules, CA) cell electrophoresis tank for 2 hr at 40 mA per gel. After separation, proteins were transferred to nitrocellulose membrane by semidry blotting for 1.5 hr at 50 mA per gel. Nonspecific binding sites were blocked by immersing the membrane in PBS (5 mM KH_2PO_4, 5 mM Na_2HPO_4, and 130 mM NaCl, pH 7.2) containing 10% (w/v) dried skimmed milk overnight at 4°C. The membrane was washed three or four times with 0.05% Tween 20 in PBS. Membranes were probed with anti-$P2X_7$ receptor primary antibody (1:1000) for 1 hr at room temperature while being agitated and then washed three times with PBS–Tween 20. Bound antibody was detected by anti-rabbit Ig conjugated to horseradish peroxidase (1:3000; Dako, Ely, UK). Immunoreactivity was visualized by using a peroxidase based chemiluminescent substrate kit (Amersham Pharmacia Biotech, Buckinghamshire, UK).

Tissue preparation for immunohistochemistry. Male Wistar rats (150–200 gm; $n = 10$) were anesthetized by intraperitoneal Sagatal (60 mg/kg) and transcardially perfused with 50 ml of heparin containing 0.9% NaCl, followed by fixative containing 4% paraformaldehyde and 0.1–0.5% glutaraldehyde in 0.1 M phosphate buffer (PB), pH 7.4. All experiments were performed under a UK Home Office License and in accordance with the regulations of the UK Animals (Scientific Procedures) Act (1986), in compliance with the National Institutes of Health and Society of Neuroscience guidelines. Medulla oblongata, spinal cord, and soleus muscle were removed and post-fixed in the same solution for 4–12 hr at 4°C. We cut 50 μm sections of the fixed tissue on a vibrating microtome (Leica, Milton Keynes, UK) and collected them into PBS, pH 7.2. Adult C57BL mice were killed by CO_2 intoxication, and transversus abdominis muscles were dissected and fixed in buffered 4% paraformaldehyde, pH 7.2.

Anterograde tracing. Vagal afferent fibers were anterogradely labeled in 150–200 gm Wistar rats ($n = 5$) under halothane anesthesia (5% in O_2) by the injection of 5–10 μl of 10% biotinylated dextran amine [BDA; molecular weight (MW) 10,000 kDa; Molecular Probes, Eugene, OR, USA) into the right nodose ganglia. After 7–10 d of recovery, the rats were anesthetized with Sagatal (60 mg/kg, i.p.) and perfused transcardially with 4% paraformaldehyde–0.1–0.5% glutaraldehyde. Sections were cut on the vibrating microtome at 50 μm and freeze-thawed in liquid nitrogen. Anterogradely transported BDA was visualized by incubating sections in ABC solution (Vector Laboratories, Peterborough, UK) for 18–20 hr at 4°C before the diaminobenzidine (DAB) reaction.

Fluorescence light microscopy. Tissue sections (rat) were obtained as described above and incubated in rabbit anti-$P2X_7$ receptor antibody as above at a concentration of 1:1000–1:5000 in PBS with 0.1% Triton X-100. After three washes for 10 min each in PBS, some sections were incubated in biotinylated secondary antibody to rabbit IgG (1:200 in PBS) for 5 hr at 4°C followed by incubation in streptavidin $Alexa^{488}$ (1:1000 in PBS; Molecular Probes) for 3 hr at room temperature. Other sections were transferred to PBS containing Cy3-conjugated anti-rabbit IgG (Jackson ImmunoResearch, Stratech, Luton, UK) at 1:1000 for 4–12 hr at room temperature. Sections were then washed three times in PBS, dried onto gelatin-coated slides at 4°C and mounted in Vectamount (Vector Laboratories) under a coverslip. Slides were viewed on a Nikon E600 microscope equipped with epifluorescence using the appropriate filter sets.

Whole mounts of transversus abdominis (mouse) were preblocked with PBS containing 1% BSA and stained *en bloc*. Postsynaptic acetylcholine receptors were labeled with tetramethylrhodamine isothiocyanate-conjugated α-bungarotoxin (TRITC-α-BTX; 5 μg/ml; Molecular Probes). $P2X_7$ receptors were labeled with primary antibody (1:1500 in 1% BSA in PBS), and visualized with fluorescein-conjugated donkey anti-rabbit secondary antibody (1:200 in 1% BSA in PBS; Scottish Antibody Production Unit, Edinburgh, UK). After three washes in PBS, whole muscles were mounted in 2.5% DABCO in glycerol.

Electron microscopy. Sections (50 μm) were cut on a vibrating microtome and cryoprotected by incubation in 10% sucrose in 0.1 M PB for 10 min followed by 20% sucrose in 0.1 M PB for 20 min and then freeze-thawed twice in liquid nitrogen to permeabilize the membranes. Sections were then incubated in rabbit anti-$P2X_7$ receptor diluted 1:5000–1:15,000 in PBS for 12–24 hr at 4°C. After three washes for 10 min each in PBS, the sections were placed into biotinylated secondary antibody to rabbit IgG diluted 1:200 in PBS (Vector Laboratories) for 5 hr at 4°C and then into Vectastain Elite ABC reagent (Vector Laboratories) for 18–20 hr at 4°C. Sections were then washed in Tris HCl buffer, pH 7.4, and incubated in DAB solution (5 mg in 10 ml of Tris HCl buffer, pH 7.4, with 0.01% H_2O_2) for 10 min. Control sections were incubated in PBS in place of primary antiserum for 12–24 hr at 4°C followed by secondary antibody and reacted with ABC–DAB as above. Other control sections were incubated for 12–24 hr at 4°C in primary antiserum for the $P2X_7$ receptor (1:5000) that had been preabsorbed with peptide antigen for 1 hr before use (1 μg of peptide for 1 μg of antibody) and then incubated in secondary antibody and reacted with ABC–DAB as above. Sections were washed in 0.1 M PB for 10 min and post-fixed in 0.5% osmium tetroxide (in 0.1 M PB) for 45 min. After washing in 0.1 M PB the sections were then dehydrated through a series of ethanols followed by two washes for 10 min each in propylene oxide (Fisher Scientific, Loughborough, UK). The sections were then immersed in Durcupan ACM resin (Fluka, Gillingham, UK) for 12–20 hr, mounted on glass slides under coverslips, and heated at 60°C for 48 hr to polymerize the resin.

Sections with anterogradely labeled vagal afferent fibers were transferred into primary antibody against the $P2X_7$ receptor (1:10,000) for 18–20 hr at 4°C, washed in PBS, and then incubated in secondary antibodies to rabbit IgG conjugated to 1 nm gold particles (Amersham Pharmacia Biotech) diluted 1:100 in PBS, pH 7.4, containing 0.8% fish gelatin and 0.1% bovine serum albumin for 18–20 hr at 4°C. After thoroughly rinsing the sections (four times for 10 min each) in distilled deionized water, the gold particles were silver-enhanced for 5–10 min using an IntenSE silver enhancement kit (Amersham Life Sciences). Sections were then osmicated and processed for electron microscopy as described above.

When areas with suitable staining for electron microscopy were selected, the coverslip was removed, and the relevant area was cut out and glued to the flat surface of a blank resin block. After trimming of the block, serial ultrathin sections (70 nm) were cut using a Leica (Nussloch, Germany) UltraCut S ultramicrotome and collected on Formvar-coated 1 mm slot grids. The sections were then stained with lead citrate before viewing on a Phillips CM10 transmission electron microscope. Negatives were digitized using an Agfa Duoscan Scanner and manipulated in Corel Draw 8/9 as below.

Image capture and manipulation. Slides were subsequently examined at the light microscope level using a Nikon E600 microscope equipped with epifluorescence and captured directly from the slide using an Acquis Image Capture System (Synoptics, Cambridge, UK). Images were ma-

nipulated in CorelDraw 8 to adjust gamma, brightness, and contrast to the desired levels.

Electrophysiology. To test whether activation of the $P2X_7R$ could influence neuronal activity in the CNS, we performed whole-cell patch-clamp recordings from neurons in the intermediolateral cell column (IML) of the spinal cord. Wistar rats aged 10–15 d were anesthetized with urethane (2 gm/kg, i.p.). The upper to middle thoracic spinal cord was exposed, isolated, and placed in ice-cold sucrose–aCSF containing (in mM) sucrose (217); $NaHCO_3$ (26); KCl (3); $MgSO_4$ (2); NaH_2PO_4 (2.5); $CaCl_2$ (1); and glucose (10) equilibrated with 95% O_2 and 5% CO_2. The dura and pia mater were removed, and the spinal cord was immersed in warm agar and placed on ice for rapid setting. Thin transverse slices (250 μm) of the embedded spinal cord were cut on a Vibroslice (Campden Instruments, Sileby, UK) and placed in the recording chamber or a holding chamber for later use. The sections were submerged in aCSF [composition (in mM): $NaCl_2$ (124); $NaHCO_3$ (26); KCl (3); $MgSO_4$ (2); NaH_2PO_4 (2.5); $CaCl_2$ (2); glucose (10)] and superfused at a rate of 3–5 ml/min. All experiments were performed at room temperature. Visualized patch-clamp recordings were performed using an upright microscope (model BX50WI; Olympus, Tokyo, Japan). The IML was located at 10× magnification, and the cells were visualized at 60× magnification for recording. Patch electrodes (tip diameter, 3 μm; resistance, 4–6 MΩ) were filled with (in mM): Kgluconate (130); KCl (10); EGTA (11); $MgCl_2$ (2); $CaCl_2$ (1); HEPES (10) Na_2GTP (0.3), and Na_2ATP (5) at pH 7.2, 295 mOsm. Neurobiotin (0.5%) was included in the patch solution and diffused into the neuron during recording. Neurons within and immediately adjacent to the IML were targeted, and whole-cell patch-clamp recordings were obtained using standard techniques. All recordings were performed in current-clamp mode using an Axopatch 1D (Axon Instruments, Foster City, CA).

To characterize the neurons electrophysiologically as sympathetic preganglionic neurons or interneurons, rectangular hyperpolarizing and depolarizing current pulses (1 sec duration, +100 to −130 pA) were applied to the neuron at a holding potential of −60 mV, and the changes in voltage were recorded. The shape of the action potential was also noted, and the duration of the action potential and amplitude of the afterhyperpolarization was measured. Neurons were then held at a resting membrane potential of −60 mV, and a small square wave depolarizing current pulse was applied (+10 to +30 pA) every 5–10 sec to monitor input resistance of the neuron. Drugs were applied to the bathing medium in the following final concentrations [agonist, 2′- and 3′-*O*-(4-benzoylbenzoyl)adenosine 5′-triphosphate 30 μM (BzATP, Sigma); antagonists, oxidized ATP, 100 μM (Sigma) and Brilliant Blue G 2 μM (Sigma)]. We used BzATP as the agonist because it is several-fold more effective than ATP at recombinant $P2X_7$ receptors (North and Surprenant, 2000). Antagonists were applied in the bathing medium for 30 min before application of the agonist.

On occasion, the excitatory amino acid antagonists NBQX (20 μM) and AP-5 (50 μM) were applied to the bathing medium to block transmission because of release of glutamate, then BzATP was added in the presence of these drugs. After washout of the NBQX and AP-5, BzATP was reapplied on its own 1.5 hr after the first application.

Visualization of nerve terminal destaining at the neuromuscular junction. Eight- to ten-week-old C57BL/6 mice were killed by inhalation of CO_2. Whole ventrolateral abdominal walls with attached lower thoracic cage were dissected in oxygenated Ringer's solution. The external oblique muscle was removed to expose underlying internal oblique and transversus abdominus musculature, which were separated in the midline to produce two hemiabdominal walls. One intercostal nerve was dissected from its intercostal space to the level of the diaphragm.

Preparations were loaded with the vital styryl dyes FM1–43 (2 μg/ml; Molecular Probes) or RH414 (10 μg/ml; Molecular Probes) in physiological saline solution by nerve stimulation (suprathreshold 0.1 msec pulse trains delivered at 10 Hz for 10 min to the intercostal nerve via a suction electrode), followed by at least 1 hr washing in oxygenated physiological saline. Preparations were transferred to the microscope stage and terminals were mapped and imaged before addition of 30 μM BzATP (Sigma). Images were captured every 5 min for 30 min, via an integrating monochrome CCD camera (Cohu, Steventon, UK), Scion (Frederick, MD) LG3 frame grabber, and an Apple Macintosh computer running Scion Image software. A 25% neutral density filter was used to attenuate the light source throughout experiments. Measurements of mean pixel intensity for regions of interest in each nerve terminal were background-subtracted and normalized to the intensity of the first image in the time sequence, to give a value of relative pixel intensity. Control preparations were imaged in an identical manner, but BzATP was omitted from the solution during imaging. In some experiments, subsequent to FM 1–43 labeling and before imaging, preparations were bathed in 100 μM oxidized ATP or 1 μM Brilliant Blue G in physiological saline for 1 hr and then transferred to 30 μM BzATP and 100 μM oxidized ATP or 1 μM Brilliant Blue G in physiological saline for imaging.

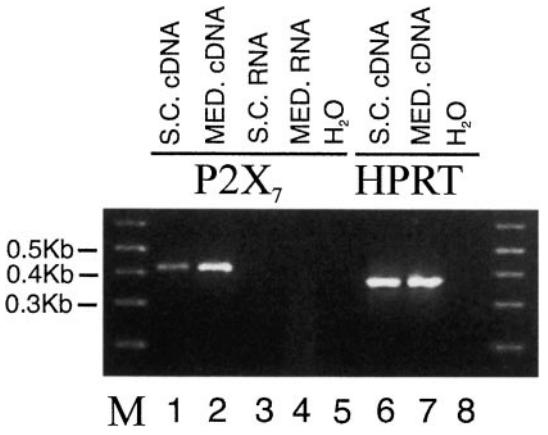

Figure 1. RT-PCR indicates expression of the $P2X_7$ receptor in spinal cord and medulla oblongata. Agarose gel electrophoresis of PCR products obtained after reverse transcription of total RNA. RT-PCR analysis revealed the presence of $P2X_7$ transcripts in RNA extracted from spinal cord (*lane 1*) and medulla (*lane 2*). No amplified products were detected when using water or RNA as template (*lanes 3*, *4*, *5*, *8*). Veracity of the amplified products was confirmed by cloning the PCR product into pGEM T-Easy followed by DNA sequencing. As a positive control, the PCR products for the housekeeping gene hprt were also detected in both tissues (*lanes 6*, *7*). Products resulting from a 1 kb molecular weight marker are indicated in *lane M,* and the bands correspond to the calculated size for all PCR products.

Dye-loading experiments. Because the $P2X_7$ receptor has been reported to open a large pore permitting nonselective passage of molecules up to 900 Da such as YO-PRO-1 (Surprenant et al., 1996), we sought to determine whether our observed responses were attributable to opening of the selectively permeable channel or the nonselective large pore. Slices of medulla oblongata and spinal cord (250 μm) were prepared as described for the electrophysiology earlier and maintained in oxygenated aCSF in glass vials at both room temperature and 35°C. The fluorescent dyes YO-PRO-1 (10 μM; MW, 629 Da; Molecular Probes) or carboxyfluorescein (40 μM; MW 376; Molecular Probes) were added to the solutions previous or simultaneous to addition of BzATP (30 μM). In some cases, oxidized ATP (100 μM) was present before BzATP was added. In other cases the excitatory amino acid receptor antagonists NBQX (20 μM) and D-APV (50 μM) were also added to the solution. As controls the fluorescent dyes were added in the absence of all drugs or in the presence of antagonists only. Slices were incubated in reaction solution for intervals between 10 and 60 min before being fixed in 4% paraformaldehyde for 60 min, resectioned at 50 μm using a vibrating microtome, and examined using filter sets appropriate to the fluorescent dye used. Similar experiments using YO-PRO-1 and carboxyfluorescein were also performed in a nerve–muscle preparation as described for the destaining experiments above.

RESULTS

mRNA encoding for the $P2X_7$ receptor is present in neurons in the CNS

RT-PCR analysis revealed the presence of $P2X_7$ transcripts in spinal cord and medulla RNA (Fig. 1, *lanes 1, 2*). No amplified products were detected when using water or RNA as template (Fig. 1*a, lanes 3*, *4, 5, 8*). Veracity of the amplified products was confirmed by cloning the PCR product into pGEM T-Easy followed by DNA sequencing. The $P2X_7$ receptor in the CNS has previously been reported to be present only in activated microglia (Collo et al., 1997), which could account for the positive PCR

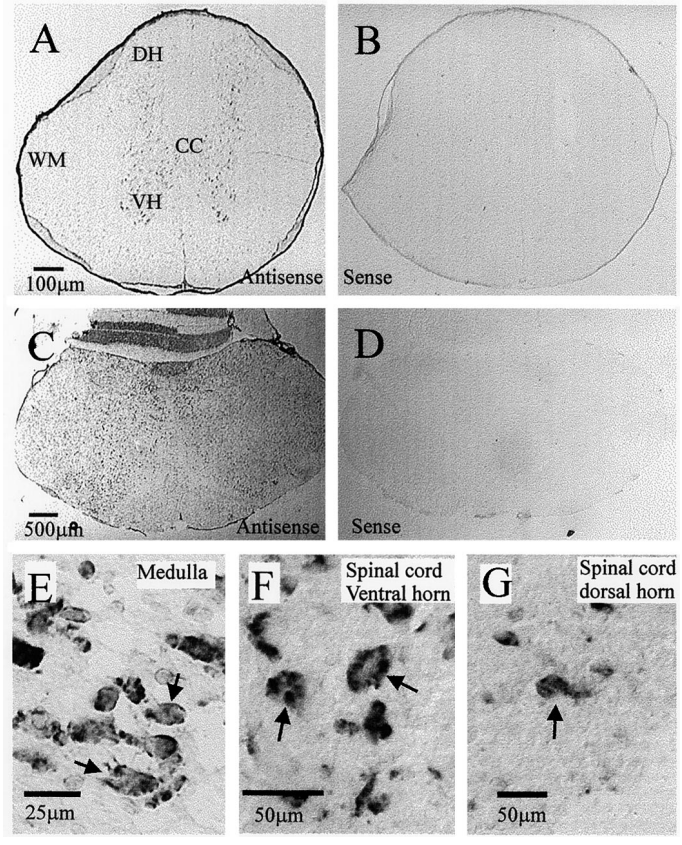

Figure 2. *In situ* hybridization reveals that messenger RNA coding for the $P2X_7$ receptor is present in neurons throughout the spinal cord and medulla oblongata. *A,* Spinal cord section indicating positive signal after hybridization with a DIG-labeled antisense probe specific to the $P2X_7$ receptor, visualized with alkaline phosphatase. The signal is present throughout the gray matter and is easily seen in the large motoneurons of the ventral horn (*VH*) as well as in dorsal horn (*DH*) neurons. The white matter (*WM*) is sparsely labeled. *B,* Spinal cord section indicating lack of signal when tissue was incubated with a sense probe to the $P2X_7$ receptor. *C,* Medulla oblongata section indicating the widespread positive signal obtained after hybridization with the DIG-labeled antisense probe specific to the $P2X_7$ receptor. Positive signal is visible in labeled neurons throughout the medulla. *D,* Medulla oblongata section indicating lack of signal when tissue was incubated with a sense probe to the $P2X_7$ receptor. *E,* Larger magnification of the dorsal vagal complex of the medulla oblongata, indicating that hybridization reaction product can be observed in neuronal structures (*arrows*). *F,* Larger magnification of the ventral horn of the spinal cord indicating that hybridization reaction product can be observed in the cytoplasm of large ventral horn motoneurons (*arrows*). *G,* Neurons (*arrow*) in the dorsal horn of the spinal cord also contain hybridization reaction product in their cytoplasm.

reaction. However, we performed *in situ* hybridization to detect $P2X_7$ mRNA, and this revealed that expression was present in the cytoplasm of neurons throughout the medulla oblongata and spinal cord (Fig. 2). A positive reaction was observed only in sections hybridized with antisense and not in sections incubated with a sense probe or without a probe.

$P2X_7$ receptor immunoreactivity is targeted to presynaptic terminals in the CNS and at the neuromuscular junction

Because *in situ* hybridization revealed neuronal expression of the $P2X_7$ receptor, we examined the cellular localization using a commercially available antibody directed toward an intracellular portion of the receptor. Evidence that the primary antibody was

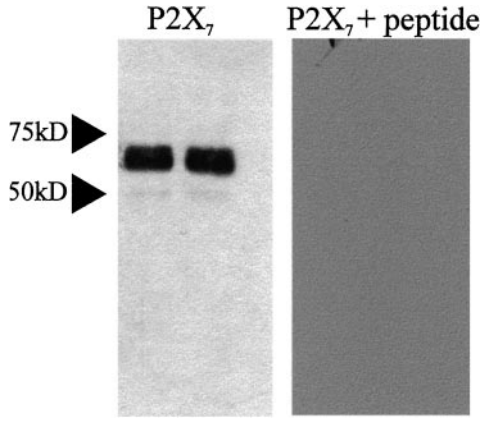

Figure 3. Western blotting indicates the tissue specificity of the antibody to $P2X_7$ receptors. Western blotting of rat brainstem resulted in staining of a major band running at ~69 kDa when detected with the anti-$P2X_7$ receptor antibody. This is the predicted molecular weight of the $P2X_7$ receptor. Preabsorption of the antiserum with the cognate peptide abolished staining of the membrane.

specific to the $P2X_7$ receptor was obtained from Western blotting, in which blotting of rat brainstem resulted in a major band at ~69 kDa (Fig. 3). This corresponds to the expected molecular weight for $P2X_7$ (Surprenant et al., 1996). Furthermore, preabsorption of the antiserum with the peptide antigen abolished staining of the membrane. This specificity appeared to be retained in tissue sections because in control sections where the primary antibody had been omitted or preabsorbed with peptide antigen, there was no staining. Furthermore, the pattern of labeling was distinct to that obtained with antibodies to the P2X subunits $P2X_2$ (Atkinson et al., 2000), $P2X_1$, and $P2X_4$ (unpublished data). Immunoreactivity for the $P2X_7$ receptor was observed in punctate structures throughout the medulla oblongata and the spinal cord with both fluorescence and transmitted light microscopy (Fig. 4). The immunoreactivity was visible in all parts of the medulla and spinal cord examined, and there was no obvious preferential localization to particular nuclei (Fig. 4). Immunoreactive structures appeared to outline the somata and dendrites of neurons (Fig. 4). Because it was not possible at the light microscopic level to determine whether these structures were glial or neuronal processes, we examined the tissue at the ultrastructural level. This electron microscopy revealed that $P2X_7$ receptor immunoreactivity was concentrated in neuronal synaptic terminals presynaptic to other neuronal structures in both the medulla oblongata and spinal cord (Fig. 5*A,B*). Synapses were characterized by the presence of clear vesicles clustered toward the presynaptic active zone, rigid apposition of presynaptic and postsynaptic membranes, and an asymmetric type (Gray's type I) thickening of the postsynaptic membrane that was often associated with subjunctional bodies (Fig. 5*A,B*). Despite examining >230 terminals in the medulla oblongata and spinal cord, we did not find any $P2X_7$-immunoreactive terminals associated with obvious symmetric (Gray's type II) synapses. In addition, the $P2X_7$ receptor was not colocalized with GABA, GAD, or the GABA vesicle transporter (vGAT) when tissue was double-stained for both antigens (data not shown). In accordance with the receptors being incorporated into the membrane, reaction product was often observed adjacent to the membrane (Fig. 5*A,B,D,E*). In addition, reaction product was present in the cytoplasm of the terminals (Fig. 5*A–E*), concordant with trafficking of the receptor to its final site or internalization after

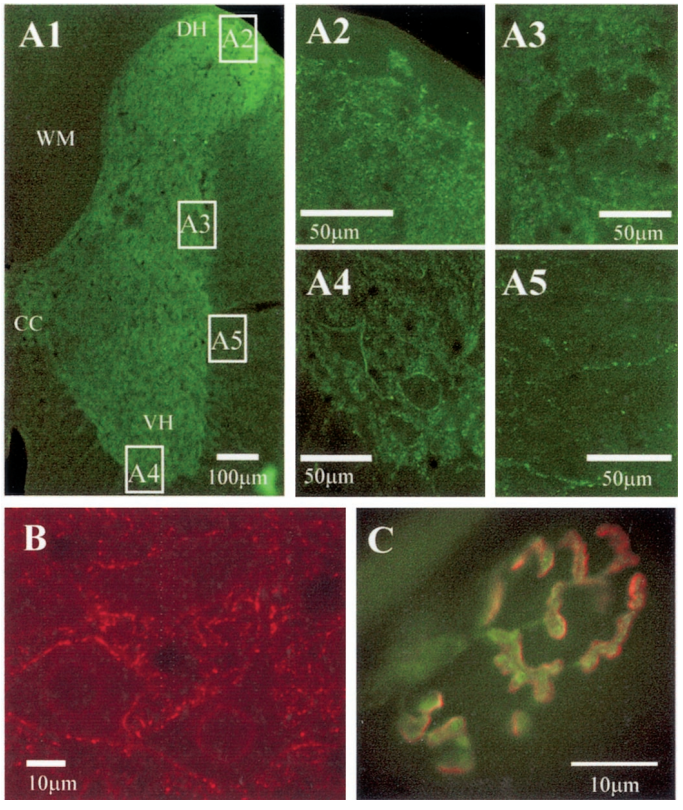

Figure 4. Widespread $P2X_7$ receptor immunoreactivity in the spinal cord, medulla oblongata, and at the neuromuscular junction is localized to punctate structures. *A1,* Half section of the spinal cord stained for $P2X_7$ immunoreactivity and detected with $Alexa^{488}$ (*green*). Labeling is dense in the neuropil of the spinal cord, but less so in the white matter. *CC,* Central canal; *VH,* central horn; *DH,* dorsal horn; *WM,* white matter. Areas indicated in *boxes* are illustrated at higher magnification as appropriate. Dense fiber staining is evident in the dorsal horn (*A2*), intermediolateral cell column (*A3*), and the ventral horn, where labeled structures appear to surround the somatic membrane of large motoneurons (*A4*). In the white matter (*A5*), occasional labeled fibers can be observed. *B,* $P2X_7$ immunoreactivity is also ubiquitous throughout the medulla oblongata. In this high-magnification view, $P2X_7$ immunoreactivity (detected with Cy3, *red*) is observed in punctate structures in the neuropil as well as surrounding the somatic membrane of neurons in the hypoglossal nucleus. *C,* Mammalian motor nerve terminals are also immunoreactive for $P2X_7$ receptors. Transversus abdominis muscle from adult mice contained $P2X_7$ receptor immunoreactivity localized to the motor nerve terminal (*green*, detected with FITC), which appear to be distinct from the postsynaptic receptors (*red*, labeled withTRITC-α-bungarotoxin).

agonist stimulation as observed in neurons transfected with GFP-tagged $P2X_1R$ (Li et al., 2000) or GFP-tagged $P2X_2R$ (Khakh et al., 2001).

Because synapses that exhibit asymmetric type morphology are considered to be excitatory in nature, we first selected terminals that we could be certain were excitatory by labeling anterogradely the central projections of vagal afferent fibers with the anterograde tracer biotinylated dextran amine. Using a procedure we have shown to be effective in localizing the $P2X_2$ receptor to vagal afferent terminals (Atkinson et al., 2000), the tracer was detected with DAB to yield an electron-dense amorphous reaction product, whereas $P2X_7$ receptor immunoreactivity was visualized by silver intensifying a gold-conjugated secondary antibody. Electron microscopic examination revealed silver deposits indicating $P2X_7$ receptor immunoreactivity in DAB-labeled myelinated fibers and terminals of central projections of vagal afferent neurons

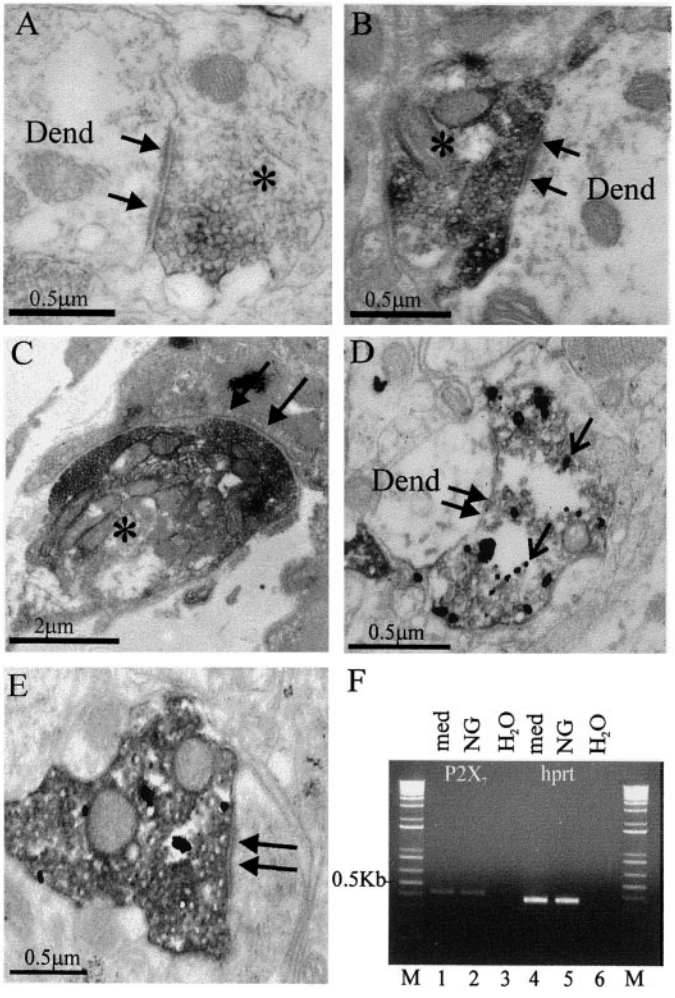

Figure 5. $P2X_7$ receptors are localized presynaptically to terminal boutons in the CNS displaying characteristics of excitatory synapses and to the motor nerve terminal at the neuromuscular junction. *A,* A presynaptic terminal (*asterisk*) in the nucleus tractus solitarius of the medulla oblongata contains electron-dense DAB reaction product (*dark gray*). The terminal forms a synapse (*arrows*) of the asymmetric type with a dendritic structure (*Dend*). *B,* A presynaptic terminal (*asterisk*) in the intermediolateral cell column of the spinal cord forms an asymmetric type synapse (*arrows*) with a dendritic structure (*Dend*). *C,* At the neuromuscular junction, immunoreactivity was also located presynaptically in the motor nerve terminal (*asterisk*). *Arrows* indicate a region of synaptic specialization at the endplate. *D,* To determine whether $P2X_7$ receptor containing terminals are excitatory, a population containing purely excitatory fibers (vagal nerve afferent fibers) was anterogradely labeled before immunohistochemistry. The electron-dense DAB labeling in this case is the result of the reaction to localize the anterograde tracer, whereas the gold deposits (*open arrow*) indicate the presence of $P2X_7$ receptor immunoreactivity in these excitatory terminals. *E,* Another example of a DAB-labeled vagal afferent terminal that contains $P2X_7$ receptor immunoreactivity. *F,* $P2X_7$ receptor mRNA was detected in the nodose ganglion, the location of the neurons giving rise to central vagal afferent projections. Agarose gel electrophoresis of PCR products obtained after reverse transcription of total RNA. RT-PCR analysis revealed the presence of $P2X_7$ transcripts in RNA extracted from medulla (*lane 1*) and nodose ganglion (*lane 2*). No amplified products were detected when using water as template (*lanes 3, 6*). As a positive control, the PCR products for the housekeeping gene hprt were also detected in both tissues (*lanes 2*, *5*). Products resulting from a 1 kb molecular weight marker are indicated in *lane M,* and the bands correspond to the calculated size for all PCR products.

($n = 10$) (Fig. 5*D,E*), indicating that the receptor is present in excitatory terminals in the CNS. Consistent with expression of the $P2X_7$ receptor in vagal sensory nerve terminals, we detected $P2X_7$ receptor transcripts in nodose ganglia extracts (Fig. 5*F*).

We did not find any $P2X_7$ receptor immunoreactivity associated with the plasma membrane of neuronal somata or dendrites, suggesting that it is not functionally targeted to the postsynaptic membrane. However, because *in situ* hybridization indicated the presence of the $P2X_7$ receptor in ventral horn motoneurons, we tested the neuromuscular junction for the presence of $P2X_7$ receptor immunoreactivity (Fig. 4*C*). Immunofluorescence microscopy indicated that punctate $P2X_7$ receptor immunoreactivity was localized to the neuromuscular junctions in neonatal and adult skeletal muscle (Fig. 4*C*). This immunoreactivity was completely blocked by preincubation with the control $P2X_7$ antigen. Electron microscopy confirmed that the $P2X_7$ immunoreactivity was located exclusively presynaptically and apparently restricted to the presynaptic face of labeled terminals (Fig. 5*C*). Notably, we found no immunoreactivity in motor nerve axons or terminal Schwann cells, but it was present in myelinating Schwann cells (data not shown). Identical preparations labeled with $P2X_1$, $P2X_2$, and $P2X_4$ antibodies (all from Alomone Labs) resulted in no labeling at the neuromuscular junction.

Activation of the $P2X_7$ receptor results in excitation of CNS neurons via release of glutamate

Because anatomical methods indicated the presence of the $P2X_7R$ in the CNS, we performed electrophysiological studies to determine whether activation of the receptor could affect neuronal activity. BzATP (30 μM) was bath-applied to 18 sympathetic preganglionic neurons recorded in the whole-cell patch-clamp configuration in spinal cord slices. After a delay for the drug to reach the tissue, there was a large depolarization of the neurons that often reached the threshold for action potential generation (Fig. 6*A*). Depolarization was sometimes so pronounced that it resulted in spike accommodation, which was maintained during the presence of the agonist (Fig. 6*A*). Because of the reported long preincubations required for antagonists to exhibit their effects (Jiang et al., 2000; North and Surprenant, 2000), we tested for antagonism by preincubating slices for 30 min in the $P2X_7$ receptor antagonists oxidized ATP (100 μM; $n = 5$) or Brilliant Blue G (2 μM; $n = 6$) and then adding BzATP. There was no response to BzATP in the presence of either antagonist. BzATP has been reported to act also on $P2X_1$ and $P2X_3$ receptors (Bianchi et al., 1999), and this can be reversibly inhibited by oxidized ATP (Evans et al., 1995). However, because oxidized ATP irreversibly inhibits the $P2X_7$ receptor (North and Surprenant, 2000), we reapplied BzATP 90 min after the first application and washout of oxidized ATP and observed no excitatory response ($n = 3$). On occasion, a reduction in firing rate of the recorded neuron was observed when BzATP was applied in the presence of antagonists (Fig. 6*B*). This may be because of unknown actions of BzATP or possible breakdown products on other receptors such as P2YR. Nevertheless, these data indicate that the receptor activated by BzATP that contributes to the excitatory response in these experiments is the $P2X_7$ receptor.

Because anatomical studies indicated that the receptor was present presynaptically in excitatory terminals, we tested the hypothesis that the observed excitation was attributable to the release of glutamate. We therefore pharmacologically antagonized ionotropic glutamate receptors by incubating slices in NBQX (20 μM) and AP-5 (50 μM) before application of BzATP

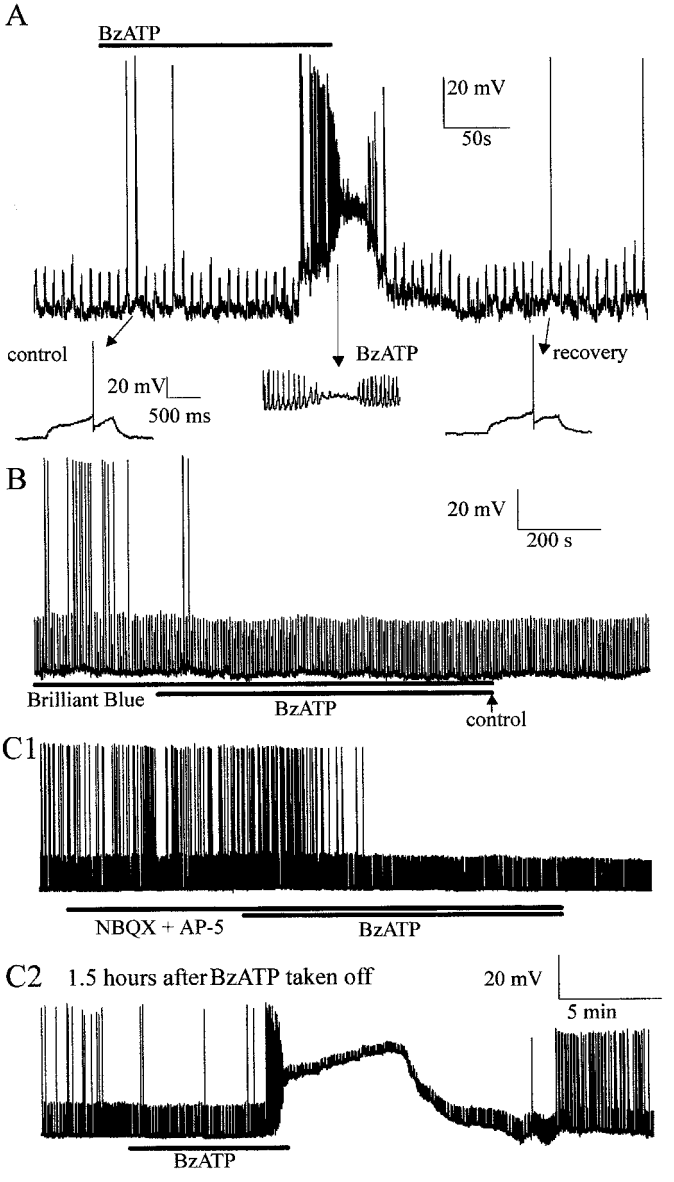

Figure 6. Activation of the $P2X_7$ receptor in CNS slices elicits depolarizations in neurons attributable to release of glutamate. *A,* The $P2X_7$ receptor agonist BzATP depolarizes neurons. In this example the cell was at a potential of −60 mV, and a depolarizing current of +20 pA, 1 sec duration was applied every 7 sec, which on occasion caused the neuron to reach the threshold for firing (shown on a faster time base below). Application of BzATP (30 μM) depolarized the neuron, resulting in discharge of action potentials and eventual depolarizing block. Recovery after washout is shown in the *inset*. *B,* The effects of BzATP were antagonized by appropriate antagonists. When preincubated in the $P2X_7$ receptor antagonist Brilliant Blue G (2 μM) for 30 min, BzATP failed to depolarize neurons. This neuron was also held at −60 mV, and depolarizing current pulses of +30 pA were applied. *C,* BzATP-evoked depolarizations were blocked by excitatory amino acid receptor antagonists. Superfusion of the non-NMDA receptor antagonist NBQX (20 μM) and the NMDA receptor antagonist AP-5 (50 μM) prevented BzATP (30 μM)-evoked depolarization even after prolonged application (*C1*). After 90 min washout, application of BzATP caused a large depolarization and increase in firing rate that again resulted in depolarizing block. This neuron was held at −60 mV with current pulses of +15 pA applied every 7 sec.

(Fig. 6*C*). When these antagonists were present, BzATP did not produce a response in the recorded neuron ($n = 3$) (Fig. 6*Ci*). However, when the antagonists were washed out and slices were allowed to recover from BzATP application for >90 min, a further application of BzATP elicited a characteristic response ($n = 2$) (Fig. 6*Cii*). These results indicate that BzATP causes release of glutamate, which excites recorded neurons.

Activation of the $P2X_7$ receptor promotes transmitter release at the neuromuscular junction

Taken together, our electrophysiological results are consistent with the anatomy and suggest an enhancement of release of transmitter through vesicular release. However, activation of the $P2X_7$ receptor has been suggested to interfere with glutamate uptake processes by transporters in Muller cells of the retina (Pannicke et al., 2000), and such reduced glutamate uptake could contribute to excitation in neurons, as observed in our experiments. We therefore tested whether activation of the $P2X_7$ receptor can result in vesicular release by direct visualization of vesicle destaining at the neuromuscular junction (Figs. 7, 8). We performed experiments in which motor nerve terminals were loaded with vital styryl dyes, which results in labeling of actively recycling vesicles. Destaining of nerve terminals is taken as evidence for vesicle exocytosis, which reflects release of neurotransmitter (Cochilla et al., 1999). In control preparations only a minimal reduction in fluorescence was observed over the 30 min visualization period (89 ± 4%; $n = 2$), which is attributed to photobleaching and spontaneous release of neurotransmitter (Figs. 7, 8). In the presence of BzATP (30 μM), nerve terminals destained with a sigmoidal time course to 48 ± 2% ($n = 6$) of their original value over the same time period (Figs. 7, 8). This is significantly different from the control preparation ($p < 0.005$; Student's *t* test). When terminals were preincubated in the $P2X_7$ receptor blockers, oxidized ATP (100 μM) or Brilliant Blue G (1 μM) terminal brightness was only reduced to 85 ± 3% ($n = 4$) and 85 ± 4% ($n = 5$), respectively (Fig. 8). These data are significantly different from the BzATP-treated preparations ($p < 0.05$; Student's *t* test) and indicate that destaining, and hence agonist-induced neurotransmitter release had been prevented. Notably, we were able to restain terminals with styryl dyes subsequent to BzATP-driven destaining, suggesting that the nerve terminals had not become damaged by the treatment.

The $P2X_7$ receptor does not undergo large pore formation in our experimental conditions

Several studies demonstrate that the activation of $P2X_7$ receptors results in the opening of a nonselective large pore permeable to molecules up to 900 Da (Steinberg and Silverstein, 1989; Surprenant et al., 1996). We therefore sought to determine whether our observed responses were caused by opening of the selectively permeable channel or the nonselective large pore. However, we were unable to demonstrate loading of terminals with YO-PRO-1 in either the neuromuscular junction or in CNS slices. We did observe YO-PRO-1 uptake by neuronal cell bodies in CNS slices, but these were also present in control tissue without agonist present and were assumed to be attributable to cell injury during tissue preparation. Because YO-PRO-1 is fluorescent only when it binds to nucleic acids, there may be insufficient nucleic acids in the terminals to make it visible. We therefore repeated the same experiments using 6-carboxyfluorescein (MW 376; 40 μM). We again did not find any staining in terminals, and the low numbers of stained neurons were similar to those observed in control experiments. We therefore suggest that activation of the $P2X_7$ receptor present in presynaptic terminals does not cause large pore formation under these experimental conditions in which the large pore might be blocked by the relatively high levels of divalent cations present (Virginio et al., 1997; Michel et al., 1999).

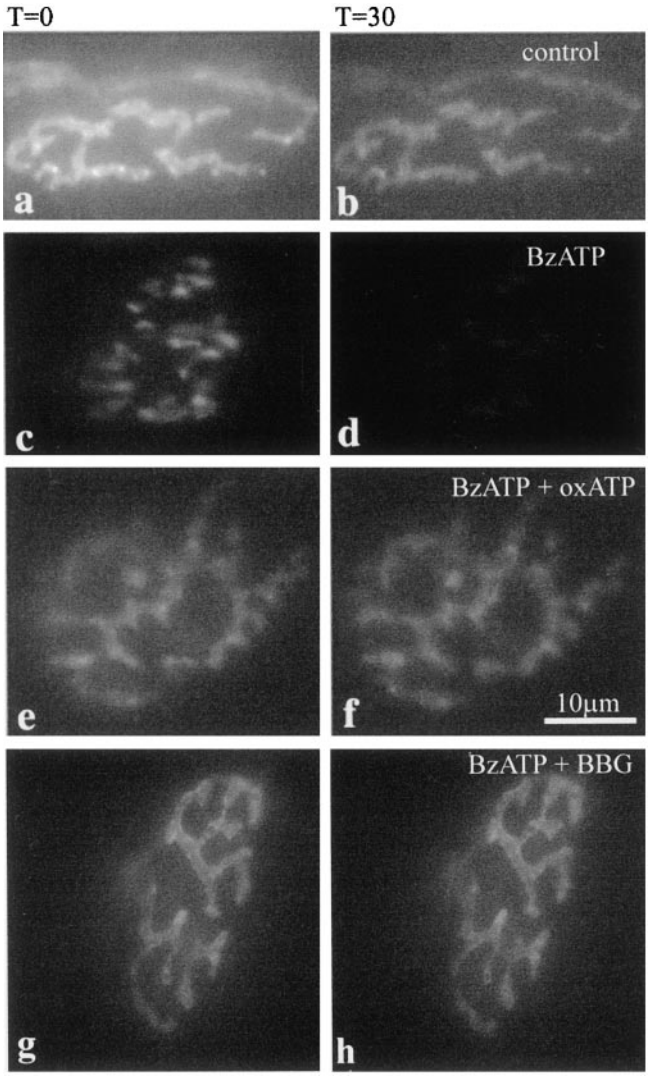

Figure 7. Activation of $P2X_7$ receptors promotes nerve terminal destaining associated with transmitter release at the neuromuscular junction. Nerve terminals were loaded with FM1–43 or RH414 and transferred to the microscope stage. Terminals were visualized, using a ND25 filter at all times, at $t = 0$ (*a, c, e*) and every 5 min until $t = 30$ min (*b, d, f*). Control preparations were repeatedly imaged and showed modest photobleaching (*a, b*). In an identical experiment but with 30 μM BzATP added at $t = 0$ (*c, d*), terminals destained by ~50%, over 30 min. In a repeat experiment in which the preparation was preincubated with 100 μM oxidized ATP (*e, f*) or 1 μM Brilliant Blue G (*g, h*) before and during BzATP addition, BzATP-mediated destaining was prevented and terminals again demonstrated some photobleaching comparable with control over 30 min.

DISCUSSION

Ionotropic ATP receptors $P2X_{1-6}$ participate in fast excitatory neurotransmission in the CNS, but to date the $P2X_7$ receptor ($P2X_7R$) has been excluded from an involvement in synaptic transmission. Here we show that the $P2X_7R$ has a remarkably widespread distribution throughout the brainstem and spinal cord where it is targeted to excitatory presynaptic terminals of neu-

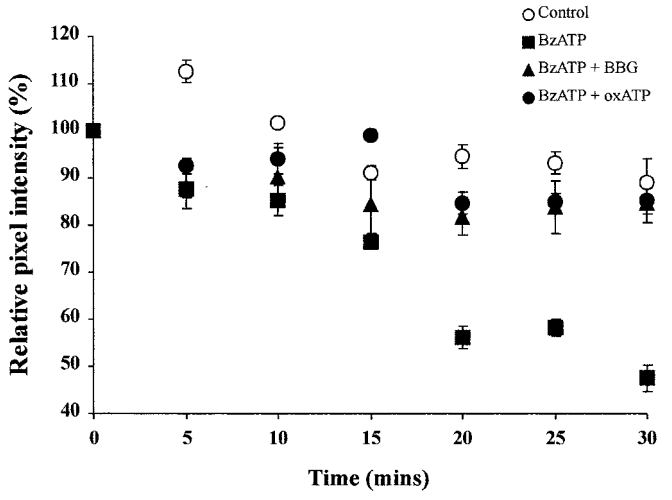

Figure 8. Quantification of P2X$_7$ receptor-mediated motor nerve terminal destaining. Plots of mean pixel intensity from multiple regions of interest on multiple nerve terminals. Values are background-subtracted and expressed as mean fractions of the value at $t = 0 \pm$ SEM. Control values (*open circles*) showed a moderate degree of photobleaching (10%). In the presence of BzATP (30 μM; *filled squares*), terminals destained by 50% over 30 min. Pretreatment with oxidized ATP (100 μM; *filled circles*) or Brilliant Blue G (1 μM; *filled triangles*) completely blocked the BzATP-evoked destain. The BzATP evoked destain is significantly different from control, oxidized ATP, or Brilliant Blue G-blocked preparations.

rons. Pharmacological activation of this receptor in CNS slices increases release of glutamate and excitation of postsynaptic neurons. At the neuromuscular junction, activation of the P2X$_7$R promotes vesicular release of neurotransmitter. These data indicate that the P2X$_7$R is functionally targeted to excitatory presynaptic terminals throughout the nervous system, where it can directly mediate and/or enhance neurotransmitter release.

Identification of the presynaptic P2X receptor as the P2X$_7$ receptor

Because the P2X$_7$R has previously been reported as absent from normal adult rat brain (Collo et al., 1997), we combined several approaches to ensure that we were indeed studying the P2X$_7$R. First, RT-PCR revealed the presence of messenger RNA for the receptor in CNS tissue. However, because a positive PCR reaction could be caused by glial cell expression, we performed *in situ* hybridization to determine the identity of the cells expressing the receptor. This procedure revealed widespread neuronal expression of the receptor in the medulla oblongata and spinal cord. Second, immunohistochemical procedures revealed specific immunoreactivity at the NMJ and in the medulla oblongata and spinal cord. The antibody used is generated against residues 576–595 of rat P2X$_7$R, a sequence not shared by any other known protein, as indicated by a BLAST database search. In addition, the C terminus of the rat P2X$_7$R is ~200 amino acids longer than other known P2XR and is not present in other known P2XR (Surprenant et al., 1996). Furthermore, Western blotting resulted in a band at the appropriate molecular weight that was abolished by preadsorption of the antibody with the antigenic peptide. These data suggest that the antibody specifically recognizes the rat P2X$_7$R. Third, our electrophysiological and destaining experiments are consistent with the activated receptor being the P2X$_7$R. We used BzATP as the agonist because it is several-fold more effective than ATP at recombinant P2X$_7$R (North and Surprenant, 2000). However, BzATP has been shown to act at recombinant P2X$_1$R with greater potency than P2X$_7$R, and at P2X$_3$R with similar potency (Bianchi et al., 1999). Nevertheless, neuronal P2X$_1$R or P2X$_3$R have not been reported in neurons in the region of the spinal cord where we conducted our electrophysiological recordings or at the NMJ. Furthermore, the BzATP responses were irreversibly blocked by oxidized ATP. Although oxidized ATP acts on P2X$_1$ and P2X$_2$ receptors, the actions on these receptors are reversible (Evans et al., 1995), whereas the action of oxidized ATP at the P2X$_7$R is irreversible (North and Surprenant, 2000). We were unable to repeat our responses after washout of oxidized ATP, consistent with an action on P2X$_7$R. In addition, Brilliant Blue G, recently reported as a selective P2X$_7$R antagonist (Jiang et al., 2000), also blocked the response to BzATP. Therefore it is likely that we have reported the results of activation of the P2X$_7$R.

Implications for synaptic transmission

Although P2X receptors have been reported to enhance or directly mediate transmitter release from presynaptic terminals (Gu and MacDermott, 1997; Khakh and Henderson, 1998; Boehm, 1999), the lack of specific agonists and antagonists have hindered identification of the particular subtypes responsible. Our findings indicate that the P2X$_7$R plays a similar role at the presynaptic terminal. However, this is the first P2XR to be conclusively identified as involved in presynaptic release because of the presence of selective agonists and antagonists for this receptor. Furthermore, the P2X$_7$R does not form heteromers with other P2X receptors in expression systems (Torres et al., 1999), and so it is likely that the native receptor exists in homomeric form.

The P2X$_7$R is considerably more prevalent at presynaptic terminals than other P2XR in the CNS. Indeed, although other P2XR are present presynaptically and postsynaptically at restricted sites in the CNS (Collo et al., 1996; Vulchanova et al., 1997; Le et al., 1998; Llewellyn-Smith and Burnstock, 1998; Loesch and Burnstock, 1998; Atkinson et al., 2000), we can only detect the P2X$_7$ receptor in presynaptic terminals. In addition, our preliminary experiments and those of Armstrong and MacVicar (2000) indicate that the P2X$_7$R is also present in excitatory presynaptic terminals in forebrain regions such as the hippocampus. Furthermore, this is the first P2 receptor to be identified at the neuromuscular junction, although ATP and its metabolites ADP and adenosine have long been known to affect synaptic transmission at the NMJ (Fu and Poo, 1991). Recently, ATP was shown to modulate neurotransmitter release from motor nerve terminals, but this was suggested to occur via an interaction with presynaptic nicotinic receptors (Salgado et al., 2000). In this light it is interesting to note that P2X$_2$ and a nicotinic receptor inhibit one another when coactivated (Khakh et al., 2000), and because we could not detect P2X$_2$ at the NMJ there is the possibility that P2X$_7$ may interact in a similar manner with presynaptic nicotinic receptors at this site.

The widespread distribution of the P2X$_7$R receptor to excitatory synaptic terminals suggests a fundamental role for the P2X$_7$R at synapses. One possible function could be as an autoreceptor, mediating positive feedback from terminals because ATP can be coreleased with other neurotransmitters (Edwards et al., 1997). At the NMJ, ATP is present in vesicles in motor nerve terminals with acetylcholine and is released into the synaptic cleft during nerve stimulation, where it can reach an estimated concentration (at least transiently) of 30–300 μM (Silinsky et al., 1990; Smith, 1991; Ribeiro et al., 1996), well within the EC$_{50}$ value of 100 μM for ATP at the rat P2X$_7$R (North and Surprenant,

2000). The prevalence of the $P2X_7R$ and the possibility that synaptically released ATP can reach sufficient levels to activate the receptor suggest that the $P2X_7R$ plays a key role in synaptic transmission.

A role for the $P2X_7$ receptor in neuropathological conditions?

Another possible role for the neuronal $P2X_7R$ is that it is activated in response to injury. In keeping with this, activation of the $P2X_7R$ evokes glutamate release, and such release is the basis of excitotoxicity (Doble, 1999). ATP is released by neurons that are damaged or under certain neuropathological conditions such as ischemia and anoxia (Dubyak and el Moatassim, 1993; Juranyi et al., 1999). Indeed, because ionic gradients collapse under anoxia and ischemia, resulting in increases in extracellular potassium levels but decreases in sodium, chloride, and calcium concentrations (Morris and Trippenbach, 1993; Xie et al., 1995; Vorisek and Sykova, 1997), $P2X_7$ receptor function might be expected to be enhanced (Virginio et al., 1997). ATP release may therefore coincide with an environment favoring activation of the $P2X_7R$. It is evident that such conditions can activate the $P2X_7R$ because the $P2X_7R$ in the brain is upregulated in tissue surrounding a necrotic region (Collo et al., 1997), and microglial cell lines contain the receptor (Ferrari et al., 1997).

After injury and associated ATP release, the neuronal $P2X_7R$ may undergo large pore formation, as observed when the $P2X_7$ receptor is exposed to agonists for prolonged periods (Steinberg and Silverstein, 1989; Ballerini et al., 1996; Surprenant et al., 1996; Chessell et al., 1997; Ferrari et al., 1997; Rassendren et al., 1997). Such large pore formation by the $P2X_7R$ has been associated with a cytolytic role (Virginio et al., 1999). We could find no evidence for large pore formation in presynaptic terminals, but there are several reasons why this might have been the case. Within the CNS slices it is possible that the high molecular weight fluorescent dyes do not gain access to the terminals, and therefore uptake cannot be observed. However, this limitation is not applicable to the neuromuscular junction where accessibility is indicated by the uptake of styryl dyes into presynaptic terminals. Another possibility is that the amount of dye entering the terminals does not provide sufficient signal for visualization. We cannot discount this possibility but note that it is possible to visualize styryl dyes in terminals. Nevertheless, the lack of large pore formation is consistent with findings when the rat $P2X_7$ receptor is expressed in oocytes (Petrou et al., 1997) and for the $P2X_7$ receptor in Muller glial cells of the human retina (Pannicke et al., 2000). Possibly the explanation lies in the relatively high concentrations of extracellular calcium and magnesium ions in our experiments because the large pore is more likely to open in low concentrations of divalent cations (Surprenant et al., 1996).

In conclusion, we show here that the $P2X_7R$ is expressed by neurons, is targeted to presynaptic terminals that are excitatory, and that activation of this receptor in the CNS and PNS elicits transmitter release, which is likely to be glutamate in the CNS. Considering the well established roles for glutamate in excitotoxicity and the activation of the $P2X_7$ receptor in response to injury, the $P2X_7$ receptor may represent a new therapeutic target to reduce cell death in times of stress.

REFERENCES

Afework M, Burnstock G (1999) Distribution of P2X receptors in the rat adrenal gland. Cell Tissue Res 298:449–456.

Armstrong JN, MacVicar BA (2000) P2X7-receptor activation depresses synaptic transmission at hippocampal mossy fiber-CA3 synapses. Soc Neurosci Abstr 26:884.

Atkinson L, Batten TF, Deuchars J (2000) P2X(2) receptor immunoreactivity in the dorsal vagal complex and area postrema of the rat. Neuroscience 99:683–696.

Ballerini P, Rathbone MP, Di Iorio P, Renzetti A, Giuliani P, D'Alimonte I, Trubiani O, Caciagli F, Ciccarelli R (1996) Rat astroglial P2Z (P2X7) receptors regulate intracellular calcium and purine release. NeuroReport 7:2533–2537.

Bardini M, Lee HY, Burnstock G (2000) Distribution of P2X receptor subtypes in the rat female reproductive tract at late pro-oestrus/early oestrus. Cell Tissue Res 299:105–113.

Bardoni R, Goldstein PA, Lee CJ, Gu JG, MacDermott AB (1997) ATP P2X receptors mediate fast synaptic transmission in the dorsal horn of the rat spinal cord. J Neurosci 17:5297–5304.

Bianchi BR, Lynch KJ, Touma E, Niforatos W, Burgard EC, Alexander KM, Park HS, Yu H, Metzger R, Kowaluk E, Jarvis MF, van Biesen T (1999) Pharmacological characterization of recombinant human and rat P2X receptor subtypes. Eur J Pharmacol 376:127–138.

Boehm S (1999) ATP stimulates sympathetic transmitter release via presynaptic P2X purinoceptors. J Neurosci 19:737–746.

Chessell IP, Michel AD, Humphrey PP (1997) Properties of the pore-forming P2X7 purinoceptor in mouse NTW8 microglial cells. Br J Pharmacol 121:1429–1437.

Chow SC, Kass GE, Orrenius S (1997) Purines and their roles in apoptosis. Neuropharmacology 36:1149–1156.

Cochilla AJ, Angleson JK, Betz WJ (1999) Monitoring secretory membrane with FM1–43 fluorescence. Annu Rev Neurosci 22:1–10.

Collo G, North RA, Kawashima E, Merlo-Pich E, Neidhart S, Surprenant A, Buell G (1996) Cloning OF P2X5 and P2X6 receptors and the distribution and properties of an extended family of ATP-gated ion channels. J Neurosci 16:2495–2507.

Collo G, Neidhart S, Kawashima E, Kosco-Vilbois M, North RA, Buell G (1997) Tissue distribution of the P2X7 receptor. Neuropharmacology 36:1277–1283.

Deuchars, J, Atkinson, L, Batten TFC, Deuchars SA Evidence that the P2X7 receptor is targetted to presynaptic terminals in the brainstem and spinal cord of rats. J Physiol (Lond) 526P, 167P. 2000.

Doble A (1999) The role of excitotoxicity in neurodegenerative disease: implications for therapy. J Pharmacol Exp Ther 81:163–221.

Dubyak GR, el Moatassim C (1993) Signal transduction via P2-purinergic receptors for extracellular ATP and other nucleotides. Am J Physiol 265:C577–C606.

Edwards FA, Robertson SJ, Gibb AJ (1997) Properties of ATP receptor-mediated synaptic transmission in the rat medial habenula. Neuropharmacology 36:1253–1268.

Evans RJ, Lewis C, Buell G, Valera S, North RA, Surprenant A (1995) Pharmacological characterization of heterologously expressed ATP-gated cation channels (P2x purinoceptors). Mol Pharmacol 48:178–183.

Ferrari D, Chiozzi P, Falzoni S, Dal Susino M, Collo G, Buell G, Di Virgilio F (1997) ATP-mediated cytotoxicity in microglial cells. Neuropharmacology 36:1295–1301.

Fu WM, Poo MM (1991) ATP potentiates spontaneous transmitter release at developing neuromuscular synapses. Neuron 6:837–843.

Gu JG, MacDermott AB (1997) Activation of ATP P2X receptors elicits glutamate release from sensory neuron synapses. Nature 389:749–753.

Hide I, Tanaka M, Inoue A, Nakajima K, Kohsaka S, Inoue K, Nakata Y (2000) Extracellular ATP triggers tumor necrosis factor-alpha release from rat microglia. J Neurochem 75:965–972.

Jiang LH, MacKenzie AB, North RA, Surprenant A (2000) Brilliant blue G selectively blocks ATP-gated rat P2X(7) receptors. Mol Pharmacol 58:82–88.

Juranyi Z, Sperlagh B, Vizi ES (1999) Involvement of P2 purinoceptors and the nitric oxide pathway in [3H]purine outflow evoked by short-term hypoxia and hypoglycemia in rat hippocampal slices. Brain Res 823:183–190.

Khakh BS, Henderson G (1998) ATP receptor-mediated enhancement of fast excitatory neurotransmitter release in the brain. Mol Pharmacol 54:372–378.

Khakh BS, Zhou X, Sydes J, Galligan JJ, Lester HA (2000) State-dependent cross-inhibition between transmitter-gated cation channels. Nature 406:405–410.

Khakh BS, Smith WB, Chiu CS, Ju D, Davidson N, Lester HA (2001) Activation-dependent changes in receptor distribution and dendritic morphology in hippocampal neurons expressing P2X2-green fluorescent protein receptors. Proc Natl Acad Sci USA 98:5288–5293.

Knutsen PM, Deuchars, J, Parson SH (2000) Immunocytochemical evidence that the P2X7 receptor is present in mammalian motor nerve terminals. J Physiol (Lond) 526:60.

Le KT, Villeneuve P, Ramjaun AR, McPherson PS, Beaudet A, Seguela P (1998) Sensory presynaptic and widespread somatodendritic immunolocalization of central ionotropic P2X ATP receptors. Neuroscience 83:177–190.

Lee HY, Bardini M, Burnstock G (2000) Distribution of P2X receptors in the urinary bladder and the ureter of the rat. J Urol 163:2002–2007.

Li GH, Lee EM, Blair D, Holding C, Poronnik P, Cook DI, Barden JA, Bennett MR (2000) The distribution of P2X receptor clusters on individual neurons in sympathetic ganglia and their redistribution on agonist activation. J Biol Chem 275:29107–29112.
Llewellyn-Smith IJ, Burnstock G (1998) Ultrastructural localization of P2X3 receptors in rat sensory neurons. NeuroReport 9:2545–2550.
Loesch A, Burnstock G (1998) Electron-immunocytochemical localization of P2X1 receptors in the rat cerebellum. Cell Tissue Res 294:253–260.
Lutz PL, Kabler S (1997) Release of adenosine and ATP in the brain of the freshwater turtle (*Trachemys scripta*) during long-term anoxia. Brain Res 769:281–286.
Michel AD, Chessell IP, Humphrey PP (1999) Ionic effects on human recombinant P2X7 receptor function. Naunyn Schmiedebergs Arch Pharmacol 359:102–109.
Morris ME, Trippenbach T (1993) Changes in extracellular [K+] and [Ca^{2+}] induced by anoxia in neonatal rabbit medulla. Am J Physiol 264:R761–R769.
Nieber K, Poelchen W, Illes P (1997) Role of ATP in fast excitatory synaptic potentials in locus coeruleus neurones of the rat. Br J Pharmacol 122:423–430.
North RA, Surprenant A (2000) Pharmacology of cloned P2X receptors. Annu Rev Pharmacol Toxicol 40:563–580.
Pankratov Y, Castro E, Miras-Portugal MT, Krishtal O (1998) A purinergic component of the excitatory postsynaptic current mediated by P2X receptors in the CA1 neurons of the rat hippocampus. Eur J Neurosci 10:3898–3902.
Pannicke T, Fischer W, Biedermann B, Schadlich H, Grosche J, Faude F, Wiedemann P, Allgaier C, Illes P, Burnstock G, Reichenbach A (2000) P2X7 receptors in Muller glial cells from the human retina. J Neurosci 20:5965–5972.
Petrou S, Ugur M, Drummond RM, Singer JJ, Walsh Jr JV (1997) P2X7 purinoceptor expression in Xenopus oocytes is not sufficient to produce a pore-forming P2Z-like phenotype. FEBS Lett 411:339–345.
Ralevic V, Burnstock G (1998) Receptors for purines and pyrimidines. Pharmacol Rev 50:413–492.
Rassendren F, Buell GN, Virginio C, Collo G, North RA, Surprenant A (1997) The permeabilizing ATP receptor, P2X7. Cloning and expression of a human cDNA. J Biol Chem 272:5482–5486.
Ribeiro JA, Cunha RA, Correia-de-Sa P, Sebastiao AM (1996) Purinergic regulation of acetylcholine release. Prog Brain Res 109:231–241.
Salgado AI, Cunha RA, Ribeiro JA (2000) Facilitation by P(2) receptor activation of acetylcholine release from rat motor nerve terminals: interaction with presynaptic nicotinic receptors. Brain Res 877:245–250.
Silinsky EM, Hunt JM, Solsona CS, Hirsh JK (1990) Prejunctional adenosine and ATP receptors. Ann NY Acad Sci 603:324–333.
Smith DO (1991) Sources of adenosine released during neuromuscular transmission in the rat. J Physiol (Lond) 432:343–354.
Steinberg TH, Silverstein SC (1989) ATP permeabilization of the plasma membrane. Methods Cell Biol 31:45–61.
Surprenant A, Rassendren F, Kawashima E, North RA, Buell G (1996) The cytolytic P2Z receptor for extracellular ATP identified as a P2X receptor (P2X7). Science 272:735–738.
Torres GE, Egan TM, Voigt MM (1999) Hetero-oligomeric assembly of P2X receptor subunits. Specificities exist with regard to possible partners. J Biol Chem 274:6653–6659.
Virginio C, Church D, North RA, Surprenant A (1997) Effects of divalent cations, protons and calmidazolium at the rat P2X7 receptor. Neuropharmacology 36:1285–1294.
Virginio C, MacKenzie A, North RA, Surprenant A (1999) Kinetics of cell lysis, dye uptake and permeability changes in cells expressing the rat P2X7 receptor. J Physiol (Lond) 519:335–346.
Vorisek I, Sykova E (1997) Ischemia-induced changes in the extracellular space diffusion parameters, K+, and pH in the developing rat cortex and corpus callosum. J Cereb Blood Flow Metab 17:191–203.
Vulchanova L, Riedl MS, Shuster SJ, Buell G, Surprenant A, North RA, Elde R (1997) Immunohistochemical study of the P2X2 and P2X3 receptor subunits in rat and monkey sensory neurons and their central terminals. Neuropharmacology 36:1229–1242.
Xie Y, Zacharias E, Hoff P, Tegtmeier F (1995) Ion channel involvement in anoxic depolarization induced by cardiac arrest in rat brain. J Cereb Blood Flow Metab 15:587–594.